Annals of Biomedical Engineering, Vol. 25, pp. 499–508, 1997
Printed in the USA. All rights reserved.

0090-6964/97 $10.50 + .00

Distribution of Contact Force during Impact to the Hip

STEPHEN N. ROBINOVITCH,* WILSON C. HAYES,* and THOMAS A. MCMAHON†

*Orthopedic Biomechanics Laboratory, Department of Orthopaedic Surgery, Charles A. Dana Research Institute, Harvard-Thorndike Laboratory, Beth Israel Hospital and Harvard Medical School, Boston, MA, and †Division of Applied Sciences, Harvard University, Cambridge, MA

Abstract—Hip fracture is a common, costly, and debilitating injury occurring primarily in the elderly. Commonly viewed as a consequence of osteoporosis, it is less often appreciated that > 90% of hip fractures are caused by falls, and that fracture risk is governed not only by bone fragility, but also by the mechanics of the fall. Our goal is to develop experimental and mathematical models that describe the dynamics of impact to the hip during a fall, and explain the factors that influence hip contact force and fracture risk during a fall. In the current study, we used "pelvis release experiments" to test the hypothesis that, during a fall on the hip, two pathways exist for energy absorption and force generation at contact: a compressive load path directly in line with the hip, and a flexural load path due to deformation of muscles and ligaments peripheral to the hip. We also explored whether trunk position or muscle contraction influence the body's impact response and the magnitude of force applied to the hip during a fall. Our results suggest that only 15% of total impact force is distributed to structures peripheral to the hip and that peak forces directly applied to the hip are well within the fracture range of the elderly femur. We also found that impacting with the trunk upright significantly increases peak force applied to the hip, whereas muscle contraction has little effect. These results should have application in the development of fracture risk indices that incorporate both fall severity and bone fragility, and the design of interventions such as hip pads and energy-absorbing floors that attempt to reduce fracture risk by decreasing in-line stiffness and hip contact force during a fall.

Keywords—Falls, Hip fracture, Impact force, Stiffness, Damping.

INTRODUCTION

Hip fractures, or fractures of the proximal femur, are an enormous health problem in the elderly, with > 280,000 cases annually and related medical costs of approximately $7 billion (9). More than 90% of hip fractures are caused by falls (4,6). Recent epidemiological studies have shown that the mechanics of the fall, as defined by the direction of the fall and location of impact, are at least as important as bone density in determining an individual's risk for hip fracture during a fall (3,7). Although biomechanics studies could clarify better the relations between fall mechanics and hip fracture risk, few studies of this type have been performed.

Our goal is to develop experimental and mathematical models that describe the dynamics of impact to the hip and explain the factors that influence hip contact force during a fall. Such force predictions could be incorporated with radiographically-derived estimates of bone strength to provide an index of a given individual's risk for hip fracture during a fall. This would allow for identification of individuals at high risk, and targeting of fall or fracture-prevention strategies, such as hip pads, exercise training, or pharmaceutical therapies, toward these individuals. Furthermore, measures of the body's impact response during a fall are essential for the development of mechanical testing systems for the design of devices such as hip pads and energy-absorbing floors (1,8,13), that attempt to reduce fracture risk by attenuating impact forces during a fall.

In a previous study, we developed an experimental technique ("pelvis-release experiments") for estimating the force applied to the hip during impact from a fall (11). The technique involved measuring the dynamic response of the body to a step change in vertical force applied to the hip, fitting a mass-spring-damper mathematical model to the measured response, and then using the model to predict impact forces occurring in corresponding falls from various heights. Whereas this earlier study provided valuable first estimates of the forces applied to the hip during a fall, it had several important limitations. First, we measured the body's total effective stiffness and damping during impact to the hip, and assumed all stiffness and damping acted through the hip joint, thus creating compressive force at the greater trochanter. This is akin to assuming all the impact energy is absorbed by the hip, rather than being partially distributed to other portions of the body. In the present study, we test the hypothesis that two pathways exist for energy absorption and force generation during impact to the hip during a fall: one directly within the hip load pathway (associated with compression of the trochan-

Acknowledgment—S. N. Robinovitch's current address is Biomechanics Laboratory, Division of Orthopedic Surgery, San Francisco General Hospital and University of California, San Francisco, CA 94110.

Address correspondence to Stephen N. Robinovitch, Biomechanics Laboratory, San Francisco General Hospital, 1001 Potrero Avenue, Room 3A36, San Francisco, CA 94110, U.S.A.

(Received 23Apr96, Revised 8Jul96, Revised, Accepted 15Jul96)

teric skin and fat, hip joint, and pelvis), and one outside the hip load pathway (associated with flexural deformations of the spine, abdominal and thoracic viscera, and muscular connections between the pelvis, trunk, and lower limb).

Second, we previously conducted experiments with subjects in a single body configuration, simulating impact to the hip with the trunk horizontal to the ground. However, subsequent studies have shown that, during a sideways-directed fall, the hip typically impacts when the trunk is in a near-vertical position (14). In the present study, we test the hypothesis that impacting the ground with the trunk in a near-horizontal location acts to increase effective mass and thereby increase the force applied to the hip at impact.

Finally, in our previous study, we assumed that when the body impacts the ground in a given configuration, its effective mass with respect to the hip is equal to the resting (or static) level of force applied to the hip in that configuration. Although such an approach followed logically from our mass-spring-damper characterization of the body, we had no means for verifying this assumption with an alternative measure of effective mass. Because our predicted impact forces were strongly influenced by the magnitude of effective mass, any errors inherent in this assumption would translate to errors in predicted impact force. In the present study, we address this limitation by developing a method to measure directly all effective mass, stiffness, and damping parameters.

METHODS

Subjects

Five males and five females participated, varying in age between 21 and 33 years [mean: 25 ± 4 (SD) years], in total body mass between 57 and 84 kg (mean: 68 ± 11 kg), and in height between 1.62 and 1.91 m (mean: 1.74 ± 0.11 m). The experiment was approved by the Harvard Faculty of Arts and Sciences Committee on the Use of Human Subjects, and informed consent was obtained from all subjects.

Human Body Model

Pelvis-release experiments measure the dynamic response of the body to a step change in vertical force applied to the hip. Perhaps the simplest model capable of simulating both the flexural and compressive deflections of the body during the experiment (and during a corresponding fall from standing height) consists of a single effective mass attached to three sets of spring-damper elements (Fig. 1). The effective moving mass is located at the hip, which is close to the center of gravity of the body when a subject is lying flat. Although it is likely that structures directly adjacent to the hip make the greatest contribution to the effective mass, any midbody segment moving with a nonzero vertical velocity during the experiment contributes to the total effective mass (just as all elements of a simply supported beam undergoing transverse vibrations contribute to its effective mass).

One spring-damper combination, consisting of elements k_c and b_c, extends vertically between the effective mass and the skin overlying the hip region. These elements represent the structural properties of the skin, fat, and muscle within the contact area, as well as the compressive properties of the proximal femur, hip joint, and pelvis. We assume that these components undergo pure vertical translation during the pelvis-release experiment. An additional set of elements, consisting of k_f and b_f, represent the combined flexural stiffness and damping of the muscles and ligaments that span the spine, and connect the pelvis to the trunk and lower limbs. These elements constrain the hip and pelvis from lateral excursions from the midline of the body. Although this is therefore a bending stiffness and damping, we express k_f and b_f as "equivalent" parameters with respect to vertical translation of the effective mass

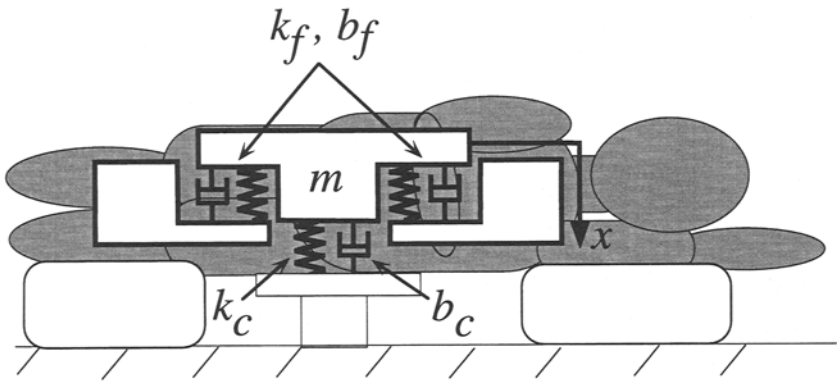

FIGURE 1. Mathematical model of the human body. Total vertical deflection (x) of the body's effective mass (m) is governed by both compressive spring-damper elements (k_c and b_c) located directly above the point of impact to the hip, and flexural spring-damper elements located peripheral to the hip (represented by the two sets of horizontally oriented spring-damper combinations, which sum to form k_f and b_f). Anatomical components that contribute to k_c and b_c include skin, fat, hip joint capsule, and pelvis. Anatomical components that contribute to k_f and b_f include the spine, and muscle and ligament connections between the trunk, pelvis, and lower extremities.

(with corresponding units N/m and N-s/m, respectively). This is similar to the common engineering practice of expressing the stiffness of a beam in lateral bending with respect to translation of its midpoint.

Experimental Protocol

Because there are five unknown parameters in our human body model, and a single step response measure (*i.e.*, pelvis-release experiment) provides only two measured quantities (the damped natural frequency ω_d and damping ratio ξ), three distinct experiments are required to characterize all model parameters. The experimental protocol used in the present study therefore involved each subject undergoing three distinct experiments (hereafter called "support conditions"), each involving measures of the body's free vibration response to a step change in vertical force applied to the hip, but distinguished by different support conditions at the hip (Fig. 2).

Support condition 1 was the "conventional" pelvis-release experiment used in our previous study (11). Subjects lay with the pelvis supported in a cloth sling having straps at the thigh and above the iliac crest, with the hip resting on a high-fidelity force platform (Sensotec Model 41/571-01, Columbus, OH, USA; natural frequency 630 rad/sec, measured from impulse response). The knees were flexed at 60°, and the contacting arm was fully ab-

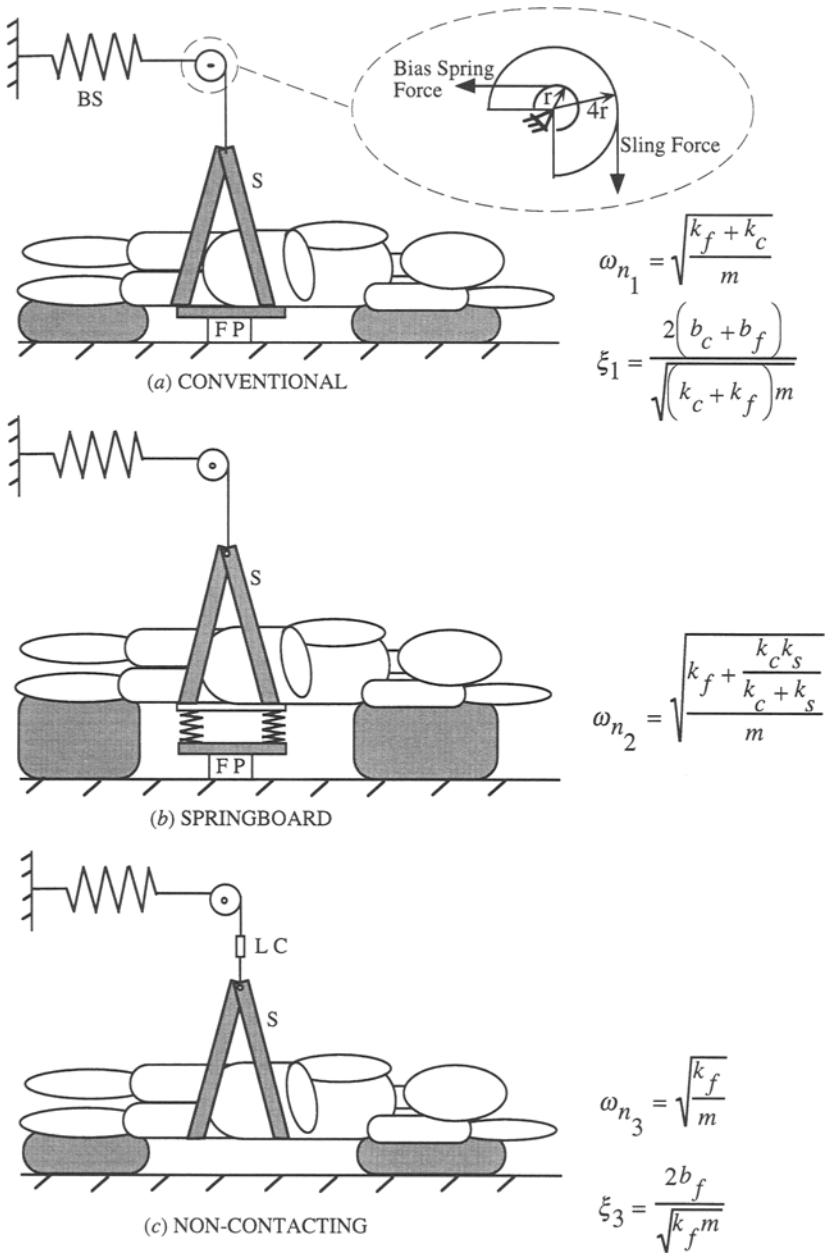

FIGURE 2. Three variations of pelvis-release experiments performed with each subject. (a) In the "conventional" support condition, the hip rested directly on the force platform (FP). (b) In the "springboard" support condition, a linear springboard of known stiffness (k_s) was placed between the hip and the force platform. (c) In the "non-contacting" support condition, the pelvic sling (S) supported the hip in midair, and the body's oscillations were measured with a load cell placed in line with the sling (LC). In the conventional and springboard experiments, both the compressive and flexural components of stiffness and damping affected the step response of the body, whereas in the noncontacting experiment, only the flexural components k_f and b_f influenced the response. Model parameters were quantified by measuring ω_n and ξ in the three support conditions, and then simultaneously solving the equations shown on the right side of the figure. The purpose of the bias spring (BS) was to adjust the resting (final) value of hip reaction force to equal 35% body weight.

ducted above the head (Fig. 2a). To ensure repeatable within-session positioning of subjects, form-fitting positional aids (Vac-Pac Model 30, Olympia Medical, Seattle, WA, USA) were placed beneath the contacting axilla and knee. The sling was rigidly connected to two overhead steel cables, which attached to pulleys of 5 cm radius. Concentrically mounted to these pulleys were two smaller pulleys of 1.25 cm radius. A steel cable connected these smaller pulleys to a steel "bias spring" of resting length 66.8 cm and stiffness 1180 N/m, which provided an essentially constant lifting force to the pelvis throughout the experiment. The entire four-pulley unit rested on a knife-edge located at the center point of the pulleys and could freely rotate on the knife-edge or by fixed in place with an electromagnetic brake (Warner Electric Co., Model PB-250, Marengo, IL, USA).

To conduct the experiment, we first adjusted the length of the sling and tension in the bias spring so the resting force applied to the hip equaled 35% of body weight. Given the difference in moment arms due to the different pulley diameters, equilibrium required the bias spring force to be 4 times the sling force. The pulley unit was then rotated counterclockwise to lift the sling ~ 1 cm, and the brake was applied to hold the pulleys stationary. The brake was then released, applying a near-step change in the vertical force applied to the pelvis (brake release time = 5.5 msec). During the resulting oscillations of the body, a measure of hip reaction force at the force platform was acquired at a sampling rate of 200 Hz for a 5-sec period.

Support condition 2, or the "springboard" support condition, was identical to the conventional experiment, except that instead of the hip resting directly on the force platform, it contacted a linear springboard of stiffness k_f placed on top of the force platform (Fig. 2b). Referring to Fig. 1, in the springboard experiment k_f is placed in series with the parallel combination of k_c and b_c. This lowers the measured frequency of vibration ω_n, and allows us to write an additional equation to solve for the unknown parameters m, k_c, k_f, b_c, and b_f (see *Parameter Identification*).

To assess the linearity of the springboard, free vibration tests were conducted at force levels between 0 to 300 N (the range of force occurring in pelvis-release experiments), achieved by placing masses in increments of 5 kg on top of the springboard, up to a maximum of 30 kg. For each value of mass, the springboard was depressed slightly by hand and released, and the frequency of ensuing vibration was averaged over 10 cycles. Springboard stiffness k_f, given by $k_f = \omega_n^2 m$, averaged 23.4 ± 0.25 kN/m, with no apparent trend between stiffness and load as assessed by linear regression.

In support condition 3, the "noncontacting" support condition, the entire body was raised several centimeters above the force platform, so that the sling supported the hip in midair (Fig. 2c). The sling force was increased (by increasing the tension on the bias spring) to ensure the body remained in the same position as during the conventional and springboard experiments. In this support condition, the step response of the body was measured with a load cell (Entran, Model ELF-TC1000-250; Fairfield, NJ, USA; 980 Hz natural frequency) inserted in-line with the sling cable.

Parameter Identification

In all experiments, the damped natural frequency ω_d and damping ratio ξ were measured from the time interval between successive peaks in force and logarithmic decrement, respectively. From these parameters, the undamped natural frequency ω_n was calculated.

In the conventional support condition, all of k_c, k_f, b_c, and b_f contributed to the measured step response. Therefore, ω_n and ξ were equal to

$$\omega_{n_1} = \sqrt{\frac{k_f^* + k_c}{m^*}} \tag{1}$$

and

$$\xi_1 = \frac{(b_f^* + b_c)}{2\sqrt{(k_f^* + k_c)m^*}} \tag{2}$$

where $m^* = m + m_{bs}$, $k_f^* = k_f + k_{bs}$, and $b_f^* = b_f + b_{bs}$, and m_{bs}, k_{bs}, and b_{bs} are the effective mass, stiffness, and damping contributed by the bias spring (Appendix 1).

In the springboard support condition, all stiffness and damping components again contributed to the response, but k_c and b_c were in series with the springboard stiffness k_s. Therefore, ω_n was equal to

$$\omega_{n_2} = \sqrt{\frac{k_f^* + \left(\frac{k_c k_s}{k_c + k_s}\right)}{m^*}}. \tag{3}$$

In the noncontacting support condition, the compressive stiffness k_c and compressive damping b_c did not influence the measured response, because the sling supported the hip in midair. The natural frequency ω_n and damping ratio ξ were therefore equal to

$$\omega_{n_3} = \sqrt{\frac{k_f^*}{m^*}} \tag{4}$$

$$\xi_3 = \frac{b_f^*}{2\sqrt{k_f^* m^*}}. \tag{5}$$

By combining Eq. 1, 3, and 4, m^* was given by

$$m^* = k_s \left[\frac{1}{(\omega_{n_2}^2 - \omega_{n_3}^2)} - \frac{1}{(\omega_{n_1}^2 - \omega_{n_3}^2)} \right], \tag{6}$$

and k_c and k_f* as

$$k_c = (\omega_{n_1}{}^2 - \omega_{n_3}{}^2)m^* \quad (7)$$

and

$$k_f^* = \omega_{n_3}{}^2 m^*. \quad (8)$$

Using Eqs. 2 and 5, b_c and b_f* were then given by

$$b_f^* = 2\xi_3 \sqrt{k_f^* m^*} \quad (9)$$

and

$$b_c = 2\xi_1 \sqrt{(k_c + k_f^*)m^*} - b_f^*. \quad (10)$$

Finally, m, k_f, and b_f were determined by subtracting the bias spring contributions:

$$m = m^* - m_{bs}, \quad (11)$$

$$k_f = k_f^* - k_{bs}, \quad (12)$$

and

$$b_f = b_f^* - b_{bs}. \quad (13)$$

Experimental Design

In addition to quantifying the mass, stiffness, and damping parameters of our human body model, we wanted to assess how muscle contraction and body position affect these parameters. Therefore, each subject underwent conventional, springboard, and noncontacting experiments in three different configurations (Fig. 3). In the "trunk-straight, muscle-relaxed" configuration, the trunk was oriented horizontally, and the subject was instructed to concentrate on relaxing all muscles. In the "trunk-straight, muscle-contracted" configuration, the trunk was again oriented horizontally, but in this case the subject was instructed to contract the abdominal and erector spinae muscles in an attempt to raise the head and contacting shoulder off the supporting platform. To ensure the resting level of hip reaction force remained at 35% of body weight, a voltmeter was used to provide visual feedback of hip reaction force to the subject. This allowed the subject to achieve the desired state of muscle contraction without bearing down at the hip. This muscle contraction scheme, which was chosen to simulate a strategy that might be used to prevent impact to the head, closely simulates the state of muscle contraction used in our previous pelvis-release experiments (11). In the "trunk-flexed, muscle-relaxed" configuration, the trunk was upright at 68° from the horizontal (matching the mean angle of the trunk found by van den Kroonenberg and coworkers (14) in measures of fall descent kinematics), the arm was outstretched to maintain balance, and the subject was instructed to concentrate on relaxing all muscles. For each of the nine total combinations of support condition and configuration, the step response measure was repeated 5 times. During the data analysis, a computer-based algorithm was used first to determine values of ω_{n_1}, ω_{n_2}, ω_{n_3}, ζ_1, ζ_2, and ζ_3 from each curve, using Eqs. 1 to 3. The algorithm then calculated average values of these parameters for each subject, and inserted these in Eqs. 6 to 13 to determine magnitudes of m, k_c, k_f, b_c, and b_f for each of the three configurations.

Fall Simulations

To predict the peak compressive and flexural forces generated during a fall from standing height, impact simulations were conducted with the model, based on values of m, k_c, k_f, b_c, and b_f measured from each subject. Simulations involved initial conditions of $x(0) = 0$ and $\dot{x}(0) = 3.0$ m/s, based on van den Kroonenberg

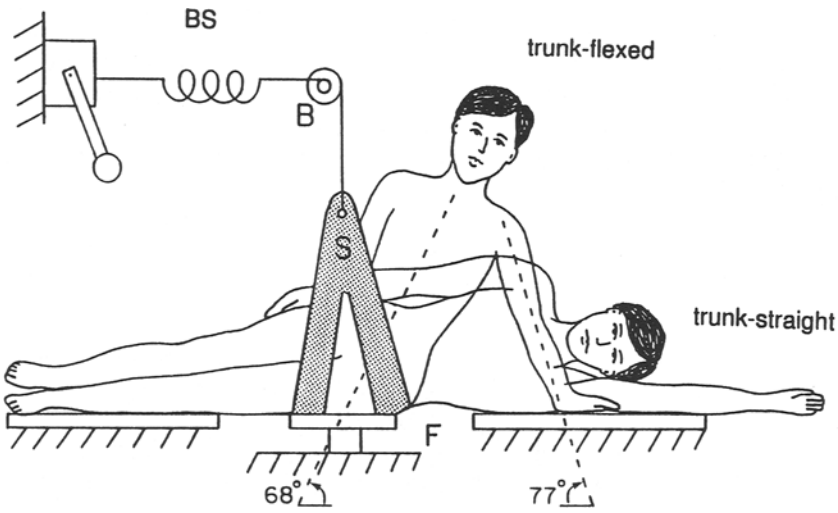

FIGURE 3. Body configurations for pelvis-release experiments. Each subject underwent conventional, springboard, and noncontacting experiments (Fig. 2) in three different configurations. In the trunk-straight, muscle-relaxed configuration, the trunk was oriented parallel with the ground, and the subject concentrated on relaxing all the muscles. In the trunk-straight, muscle-contracted configuration, the trunk was again parallel with the ground, and the subject contracted the erector spinae and abdominal muscles in an attempt to raise the head and shoulder off the underlying platform (simulating a protective response to prevent head impact during a fall). In the trunk-flexed configuration, the trunk was upright at an angle of 68° to the horizontal, matching the average orientation of the trunk at impact measured from the fall kinematics experiments of van den Kroonenberg and coworkers (14).

and coworkers (14) measures of hip impact velocity in experimental falls. Compressive force was given by $F_c = k_c x + b_c \dot{x}$, and flexural force was given by $F_f = k_f x + b_f \dot{x}$.

Statistical Analysis

To assess within-session repeatability, we examined the coefficient of variation (defined as the standard deviation of the measure divided by the mean) of ω_n and ξ in each of the nine series of experiments conducted with each subject. To assess whether trunk configuration at impact or the state of muscle contraction affected the observed magnitudes of m, k_c, k_f, b_c, or b_f, we performed a one-way, repeated-measures analysis of variance.

RESULTS

In all experiments, the response of the body was dominated by a single frequency of vibration ω_n (Fig. 4). In the conventional experiment, average values of ω_n varied from 36 to 39 rad/sec, whereas average values of ξ varied from 0.17 to 0.29. In the springboard experiment, average values of ω_n varied from 24 to 25 rad/sec, whereas average values of ξ varied from 0.11 to 0.17. In the noncontacting experiment, average values of ω_n varied from 12 to 15 rad/sec, whereas average values of ξ varied from 0.14 to 0.23.

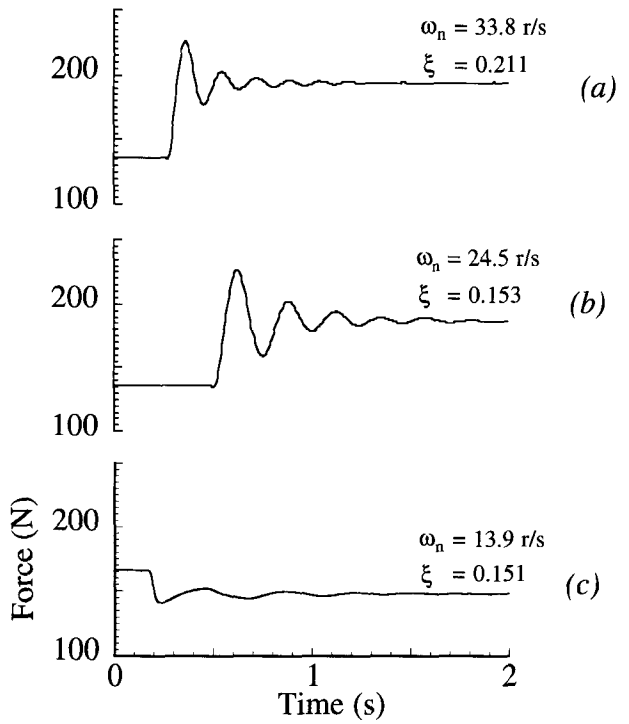

FIGURE 4. Typical variations in hip reaction force during pelvis-release experiments (subject: f3). Force records (a), (b), and (c) correspond to the three variations of the pelvis-release experiment (a), (b), and (c) shown in Fig. 2. The measured natural frequency of the body was highest in the conventional support condition and lowest in the noncontacting support condition. In all cases, the oscillatory decay was typical of a damped single-degree-of-freedom system.

Values for m, k_c, k_f, b_c, and b_f for each subject are given in Table 1, where the three numbers in each cell correspond to values obtained in configurations 1, 2, and 3, respectively (male subjects are denoted m1 to m5, whereas female subjects are denoted f1 to f5). Also shown are peak compressive (F_c) and flexural (F_f) forces calculated by the impact model for standing-height falls. Table 2 displays average values for these parameters.

Analysis of variance revealed that effective mass m did not vary significantly with impact configuration (Tables 1 and 2). Compressive stiffness k_c was significantly higher in the trunk-flexed configuration than in the two trunk-straight configurations ($p = 0.01$), whereas compressive damping b_c was significantly lower in the trunk-flexed configuration than in trunk-straight configurations ($p = 0.03$). Average contributions of k_f and b_f to total effective stiffness and damping were $14 \pm 5\%$ and $24 \pm 18\%$, respectively. The effect of impact configuration on both k_f and b_f was not significant.

Peak predicted compressive forces during simulated falls standing height varied from 1,145 to 4,921 N, and were significantly greater ($p = 0.03$) in configuration 3 than in configurations 1 and 2 (Tables 1 and 2). Peak flexural forces were much lower than peak compressive forces, ranging from 181 to 983 N. Flexural forces did not change significantly between impact configurations. The ratio of peak flexural force to peak total (compressive + flexural) force varied between 0.06 and 0.23, averaging 0.15 ± 0.04 for configuration 1, 0.16 ± 0.03 for configuration 2, and 0.11 ± 0.04 for configuration 3.

In configuration 1, body weight significantly and positively correlated with all variables except k_c (Table 1). However, in configurations 2 and 3, body weight did not influence any of the model parameters. At present, we are unable to explain fully the reasons for this discrepancy. It may be that subtle differences existed in the techniques subjects used to achieve the muscle-contracted state, or support the body in the trunk-flexed position, and such variations masked any effect body weight might have otherwise supplied. In any case, our numbers of subjects tested, although adequate to assess how trunk configuration and muscle contraction affected the body's impact response using a repeated-measures design, prevents us from making strong conclusions regarding the effect of gender or body weight on the body's impact response.

Whereas we observed significant between-subject variations in mass, stiffness, and damping (Table 1), within-subject repeatability (the relevant index of repeatability for a repeated-measures design) was high, as measured by the average coefficient of variation between the

TABLE 1. Parameter values and predicted impact forces for each subject.

Subject	Body Mass (kg)	m (kg)[a]	k_c (kN/m)[a]	k_f (kN/m)[a]	b_c (N-s/m)[a]	b_f (N-s/m)[a]	F_c (N)[b]	F_f (N)[b]
		59.0	70.0	16.6	1380	219	4920	983
m1	82.8	29.2	46.8	8.3	899	89	2970	387
		35.7	49.7	6.4	292	318	2970	615
		26.2	23.7	6.3	187	146	1830	557
m2	61.2	15.9	13.9	4.7	215	130	1150	309
		32.3	62.2	5.0	312	225	3470	421
		41.4	45.8	9.8	1070	58	3560	440
m3	81.2	25.9	22.3	5.1	287	54	1850	409
		38.6	51.4	3.4	13	65	3670	272
		40.1	46.3	11.2	175	175	3180	752
m4	71.3	37.4	32.6	9.0	711	91	2680	573
		57.5	59.0	10.9	629	249	4360	932
		41.6	64.2	7.8	1059	168	1960	545
m5	83.9	45.8	50.9	8.8	703	247	3530	858
		46.9	66.0	3.7	364	158	5288	297
		26.2	29.0	5.5	439	31	2140	341
f1	63.0	32.7	36.0	7.3	609	38	2660	426
		42.0	65.4	8.3	320	256	4530	625
		27.7	27.3	4.3	522	91	2100	342
f2	61.3	51.5	48.9	8.7	1233	105	4100	509
		34.9	43.2	2.8	664	121	2990	298
		34.2	34.2	6.7	421	53	2660	490
f3	59.0	50.1	55.1	11.3	889	156	3950	776
		48.5	60.1	7.6	529	135	4250	597
		24.2	34.4	4.6	230	132	2210	375
f4	58.2	20.1	30.0	4.4	224	136	1820	357
		34.7	61.6	7.7	13	98	4210	535
		24.4	27.3	4.3	324	58	1992	321
f5	57.2	19.2	17.0	3.6	207	47	1452	271
		16.4	17.5	2.0	56	27	1503	181

[a]Cell entries correspond to values for configurations 1, 2, and 3, respectively.
[b]Impact forces are based on an impact velocity of 3 m/sec.

five repeated measures conducted for each experimental series (0.0482 for ω_n and 0.286 for ξ).

DISCUSSION

Our results suggest that for the impact position we examined, the body oscillates like an underdamped, simply supported beam in its first mode of vibration, with an effective mass close to one-half total body mass (the analytic result for a simply supported beam with uniformly distributed mass). The flexural stiffness and damping of the body (provided by the spine, and muscle and ligament connections between pelvis, trunk, and lower extremity) have secondary roles in influencing the frequency and amplitude of the response. Rather, this response is dominated by compressive stiffness and damping components directly in-line with the hip load vector (pelvis, hip joint capsule, skin, fat, and muscle overlying hip), which are 7.0 and 5.9 times greater in magnitude, respectively, than flexural parameters. Consequently, compressive forces generated at the hip during a standing-height fall are on average

TABLE 2. Average parameter values and predicted impact forces

Configuration	m (kg)	k_c (kN/m)	k_f (kN/m)	b_c (N-s/m)	b_f (N-s/m)	F_c (kN)[a]	F_f (kN)[a]
1	34.5 ± 11.2	40.2 ± 16.1	7.70 ± 3.91	640 ± 408	113.2 ± 63.6	2.85 ± 1.02	0.52 ± 0.21
2	32.8 ± 13.0	35.4 ± 14.7	7.12 ± 2.53	598 ± 356	88.2 ± 78.6	2.62 ± 1.03	0.48 ± 0.18
3	38.8 ± 11.1	53.6 ± 14.6	5.77 ± 2.87	322 ± 258	166.1 ± 99.2	3.56 ± 0.95	0.50 ± 0.23

[a]Impact forces are based on an impact velocity of 3 m/sec.

5.8 times greater than flexural forces generated by peripheral load-bearing elements.

We found that contacting with the trunk flexed significantly increased the magnitude of k_c and the predicted peak force applied to the hip during a fall. This increased stiffness is perhaps due to changes in the geometrical relations between femur, pelvis, and supporting ligaments in the trunk-flexed position. Because increasing the angle of the trunk from the straight to flexed position places the large trunk mass closer to the hip, we expected m to increase in the trunk-flexed position. The most probable explanation for why a significant increase in m did not occur is the effect of the outstretched arm in fixing a portion of the trunk mass stationary, and preventing it from contributing to effective mass. Extending our vibrating-beam analogy, the body in the trunk-flexed position stimulates a curved beam, with vertical motion constraints at the knee and shoulder. Although the effect of removing the shoulder constraint (*i.e.,* impacting without the outstretched arm contacting before the hip) should be to increase effective mass (and thus increase contact forces), we cannot confirm this from the results of the present study.

We found that the state of muscle contraction at impact had little effect on effective mass, stiffness, and damping parameters, as well as predicted impact forces for a standing-height fall. This result is in contrast with our previous findings (11) that muscle contraction increases effective mass, stiffness, and damping. This discrepancy is most likely due to different methods for determining the effective mass of the body. In our previous study, m was estimated from the resting level of force applied to the hip when the lifting force of the pelvic sling was zero. Subjects tended to bear down at the hip when assuming the muscle-contracted state, and this caused an increase in the resting magnitude of hip reaction force. This increase in hip reaction force was then interpreted as an increase in m, and subsequently gave rise to related increases in k and b (see Eqs. 10 to 13). The present study shows, through a direct measure of m, that when similar muscle contraction of the abdominal oblique and erector spinae muscles occurs, but bearing down at the hip is prevented, effective mass does not increase. Although it is unlikely that bearing down at the hip alone (without a significant change in body configuration) should increase effective mass, our present results seem to correct the error inherent in our previous method to estimate m.

To facilitate measurement of both flexural and compressive components of stiffness and damping, we have used a fairly simple model of impact, which consists of parallel spring-damper arrangements, sometimes referred to as Voigt or Kelvin solids. A limitation of this model in describing impact behavior is its prediction of an instantaneous compressive force at impact (of magnitude $b_c u$). Although in this regard, a preferable model of impact might, for example, consists of a three-parameter solid (where b_c is replaced with a series spring-damper arrangement), we have found in validation tests that such modifications actually provide a rather small improvement in the ability of the model to predict impact force (10) and therefore do not necessarily warrant the additional computational effort involved in their use.

Two methods are available for studying the impact response of the body during a fall: cadaveric studies and studies with living humans. Both approaches have their strengths and weaknesses. The chief advantage of a cadaver-based study would be the ability to subject the cadaver to impact loads and energies representative of those occurring in real-life falls, thus eliminating the extrapolation process involved in the present study. However, the impact response of a cadaver may significantly differ from a living human, due to lack of neuromuscular reflexes, postmortem changes in the skin and fat overlying the hip region, and changes in the passive properties of muscles spanning the joints due to rigor or other postmortem processes. Moreover, a cadaver-based study of hip impact would very likely require that kinematic constraints be applied to the body to "prop" it into the configuration of interest, and such constraints would likely affect the dynamic response. For example, obtaining our trunk-flexed configuration with cadavera would require tethers and/or braces at the elbow and shoulder to provide the desired trunk inclination and load bearing at the upper extremity. It would be difficult if not impossible to account for the effect of such bracing on the measured response.

By using living humans in our study, we removed the need to impose artificial kinematic constraints on the body, and were able to account for muscle reflexes and physiological soft tissue properties. However, our experiments could be performed only at safe loading levels (*i.e.,* hip reaction forces equal to 35% body weight or a mean force level of 230 N), and due to the nonlinear force-deflection and force-velocity properties of biological tissues, a fundamental question is whether the response of the body at these low forces is representative of that occurring in an actual fall. Insight into this issue can be obtained by examining the results of a previous study, where we measured the impact response of subjects during pelvis-release experiments conducted at force levels between ~10 and 50% body weight (11). As expected, we found that the total effective stiffness and damping of the body increased as the force level of the experiment increased. However, the nonlinear portion of these relations was largely confined to the low force regime, and, on average, stiffness and damping constants reached 82 and 90% of their final predicted values, respectively, by 230 N force. This suggests that our experiments at hip reaction force levels equal to 35% of body weight provide stiffness

and damping measures that closely match the values expected to dominate the response of the body in an actual fall.

An important assumption in our impact model is that, during contact to the hip from an actual fall, the body exhibits a single mode shape that is similar in nature to the pattern of vibration observed during pelvis-release experiments. It seems that during our experiments, the body vibrates in what is likely to be its lowest mode (with a frequency of ~37 rad/sec, or 6 Hz). No secondary frequencies were evident in our force signals, which, if present, would indicate a system possessing multiple modes of vibration. We therefore expect that during an actual fall, the body's impact response will be governed by a mode similar to what we have measured.

Furthermore, we focused on a specific falling situation, involving impact to the hip after contact occurs to the shin and arm (and impact transients applied to these regions have decayed to negligible levels). An apparently more complex situation arises if impact occurs to the hip simultaneously (or just before) impact to other body parts, because the inertia, stiffness, damping, and impact velocity of all contacting regions may influence contact forces. Experimental measures of the dynamics involved in such falls could be obtained by having the sling lift and release the entire body, not just the pelvis. Modifications to our mathematical model would also be suggested, involving replacement of the rigid couplings between ground and extremities in Fig. 1 with compressive spring-dampers. However, a simpler representation of such falls is implied by the present study's demonstration of a relatively weak coupling between the pelvis, lower extremities, and trunk (*i.e.,* low magnitude of k_f and b_f). If this coupling remains weak for any sideways fall, the force applied to the pelvis will be dominated by the magnitudes of m, k_c, b_c, and the impact velocity of m. In this case, the pelvic contact forces reported in the present study may well apply to any fall on the hip, regardless of whether the hip is the first body segment to impact the ground.

It is important to consider the applicability of our results, which are based on measures of the impact response of young, healthy subjects to elderly subjects who are at greatest risk for falling and suffering hip fracture. Elderly individuals would undoubtedly represent the most appropriate subjects for this experiment, if not for the chance that even the relatively small loads involved in the experiments (< 500 N) might be sufficient to fracture an osteoporotic hip (5). However, in our opinion, no reason exists why age alone should affect the impact response of the body and the loads generated at the hip during a fall. Rather, this response will be influenced by factors such as impact configuration, the state of muscle contraction at impact, the faller's body mass and body habitus, and the thickness of soft tissues overlying the hip region. Our approach in the current and previous (11) studies has therefore been to examine how these parameters, rather than age, influence the body's impact response and the related risk for hip fracture.

In summary, the results of the current study show that, during impact to the hip from a fall, the proximal femur region absorbs the vast majority of force and impact energy; only ~15% of the total impact force is applied to structures peripheral to the hip. Predicted hip impact forces, that vary between 1,145 and 5,288 N, are well within the range of force previously found to fracture the elderly cadaveric femur (2,5). Impacting the ground with the trunk upright significantly increases peak force applied to the hip, whereas muscle contraction has little effect. These data should have application in the development of fracture risk indices that incorporate both fall severity and bone fragility, and the design of interventions such as hip pads and energy-absorbing floors that attempt to reduce fracture risk by decreasing in-line stiffness and hip contact force during a fall.

REFERENCES

1. Casalena, J. A., A. Badre-Alam, T. C. Ovaert, P. R. Cavanagh, and D. A. Streit. A dual stiffness floor for the reduction of fall injuries: finite element analysis and design. In: Proceedings of the 4th Annual CDC Injury Prevention through Biomechanics Symposium, edited by S. J. Shieh. Detroit: Wayne State University, 1994, pp. 21–25.
2. Courtney, A. C., E. F. Wachtel, B. R. Myers, and W. C. Hayes. Effects of loading rate on strength of the proximal femur. *Calc. Tissue Int.* 55:53–8, 1994.
3. Greenspan, S. L., E. R. Myers, L. A. Maitland, N. M. Resnick, and W. C. Hayes. Fall severity and bone mineral density as risk factors for hip fracture in ambulatory elderly. *J.A.M.A.* 271:128–133, 1994.
4. Grisso, J. A., J. L. Kelsey, B. L. Strom, G. Y. Chiu, *et al.* Risk factors for falls as a cause of hip fracture in women. *N. Engl. J. Med.* 324:1326–1331, 1991.
5. Lotz, J. C., and W. C. Hayes. Estimates of hip fracture risk from falls using quantitative computed tomography. *J. Bone Joint Surg. [Am.]* 72:689–700, 1990.
6. Melton, L. J., E. Y. S. Chao, and J. Lane. Biomechanical aspects of fractures. In Osteoporosis: etiology, diagnosis, and management, edited by B. L. Riggs and L. J. Melton. New York: Raven Press, 1988, pp. 111–131.
7. Nevitt, M. C., and S. R. Cummings. Type of fall and risk of hip and wrist fractures: the study of osteoporotic fractures. *J. Am. Geriatr. Soc.* 41:1226–1234, 1993.
8. Parkkari, J., P. Kannus, J. Poutala, and I. Vuori. Force attenuation properties of various trochanteric padding materials under typical falling conditions of the elderly. *J. Bone Miner. Res.* 9:1391–1396, 1994.
9. Praemer, A., S. Furner, and D. P. Rice. Musculoskeletal Conditions in the United States. Park Ridge, IL: American Academy of Orthopaedic Surgeons, 1992.
10. Robinovitch, S. N. Hip fracture and fall impact biomechanics. Cambridge, MA: Harvard/M.I.T., Division of Health, Science, and Technology, Ph.D. Thesis, 1994.
11. Robinovitch, S. N., W. C. Hayes, and T. A. McMahon. Pre-

diction of femoral impact forces in falls on the hip. *J. Biomech. Eng.* 113:366–374, 1991.
12. Robinovitch, S. N., T. A. McMahon, and W. C. Hayes. Force attenuation in trochanteric soft tissues during impact from a fall. *J. Orthop. Res.* 13:956–962, 1995.
13. Robinovitch, S. N., T. A. McMahon, and W. C. Hayes. Energy-shunting hip padding system attenuates femoral impact force in a simulated fall. *J. Biomech. Eng.* 117:409–413, 1995.
14. van den Kroonenberg, A., W. C. Hayes, and T. A. McMahon. Hip impact velocities and body configurations for experimental falls from standing height. *J. Biomech.* 29:807–811, 1996.

APPENDIX A: MEASURE OF BIAS SPRING MASS AND STIFFNESS

To measure how the bias spring influenced the measured step response, we conducted experiments where the human body was replaced in the pelvis-release apparatus with a system consisting of a steel weight supported on a springboard constructed of four linear steel springs. The stiffness of the springboard was k = 64,243 N/m (measured from the step response), and experiments were conducted with weights of mass m_1 = 27.9 kg and m_2 = 42.3 kg. When placed on top of the force platform without the sling attached and tapped, these mass-spring systems would vibrate for several minutes if undisturbed, showing that damping in the springs was negligible.

In these experiments, the protocol consisted of attaching the sling and bias spring to the steel weight, adjusting the bias spring tension to lift off 200 N of weight, and conducting three repeated measures of the system's step response. Because the bias spring stiffness k_{bs} and damping b_{bs} act in parallel with k_s, and the bias spring mass m_{bs} acts as if lumped with m_s, the natural frequency ω_n of the system was equal to

$$\omega_{n_1} = \sqrt{\frac{k_1 + k_{bs}}{m_1 + m_{bs}}} \tag{A1}$$

and

$$\omega_{n_2} = \sqrt{\frac{k + k_{bs}}{m_2 + m_{bs}}}. \tag{A2}$$

Combining Eqs. A1 and A2, the mass and stiffness of the bias spring were given by

$$m_{bs} = \frac{m_1\omega_{n_1}^2 - m_2\omega_{n_2}^2}{\omega_{n_2}^2 - \omega_{n_1}^2} \tag{A3}$$

and

$$k_{bs} = \omega_{n_1}{}^2 (m_1 + m_{bs}) - k. \tag{A4}$$

The damping constant of the bias spring was then given by

$$b_{bs} = 2\xi_1\ \omega_{n_1}(m_1 + m_{bs}). \tag{A5}$$

We found that, for the $m_1 - k$ system, ω_{n_1} = 47.5 ± 0.066 (SD) rad/sec, and ξ_1 = 0.0187 ± 0.0016. For the $m_2 - k$ system, ω_{n_2} = 38.7 ± 0.045 rad/sec, and ξ_2 = 0.0244 ± 0.00206. Using these values in Eqs. A3 to A5, m_{bs} = 0.655 kg, k_{bs} = 187 N/m, and b_{bs} = 50.9 N-s/m.